OPEN JOURNAL SYSTEMS
ISSN:2237-2202

Available on line at Directory of Open Access Journals
Journal of Hyperspectral Remote Sensing v.10, n.3 (2020) 130-137

www.periodicos.ufpe.br/revistas/jhrs

Journal of Hyperspectral Remote Sensing
www.ufpe.br/jhrs

Soil classes separation applying Principal Component Analysis (PCA)

Valéria R. Lourenço[*], David B. de S. Teixeira[**], Carlos A. G. Costa[***], Carlos A. K. Taniguchi[****]

[*]Empresa de Assistência Técnica e Extensão Rural do Ceará (Ematerce). Fortaleza-CE, Brazil.
Email: ramos.valeria74@yahoo.com (Corresponding author)
[**]Universidade Federal de Viçosa (UFV). Viçosa-MG, Brazil. Email: david.teixeira@ufv.br
[***]Universidade Federal do Ceará (UFC). Fortaleza-CE, Brazil. Email: costacag@gmail.com
[****]Empresa Brasileira de Pesquisa Agropecuária (Embrapa Agroindústria Tropical). Fortaleza-CE, Brazil. Email: carlos.taniguchi@embrapa.br

Received 18 May 2020; accepted 9 December 2020

Abstract

The spectrally active components of the soil allow the realization of integrative analyzes of soil aspects such as their classification. The purpose of this study was to evaluate the separation of soil classes from spectral reflectance data using principal components analysis (PCA). The study was carried out in the Aiuaba Experimental Basin located in the municipality of Aiuaba, Ceará, Brazil. Soil samples were collected in Ustalfs, Ustults, and Ustorthents profiles. The samples were submitted to spectral analysis by a spectroradiometer and, subsequently, to PCA. Principal components were used to identify which of them contribute more significantly to the separation of the soil classes analyzed, based on their relationship with the soil attributes using a two-dimensional graphical analysis. From the examination of spectral behavior data of the different soil classes, the use of PCA allowed the separation of the classes Ustorthents, Ustalfs, and Ustults from each other.
Keywords: ustalfs; ustults; ustorthents; reflectance, spectroradiometer.

1. Introduction

Due to the exponential growth in data availability in several study areas, a new age of information processing, the big data, has started, with which new needs are raised, such as the processing capacity of these data. Facing this, there were proposed processing techniques and algorithms that aim to meet this need, and that can return valuable information from this data density (Jollife and Cadima, 2016; Wu et al., 2018).

In the field of soil science, the great variability of soils and its attributes have always involved large databases and, with the advent of new technologies that make it easier to acquire, this characteristic is more and more prominent. Studies that depart from surveys using orbital (Mendonça-Santos et al., 2010; Liddicoat et al., 2015; Laborczi et al., 2016; Kalambukattu et al., 2018) or proximal sensors, such as those of Cheng et al. (2019) that estimated the concentration of heavy metals in the soil correlating the spectra of these elements with their reflectance, or Curcio et al. (2013) that predicted textural classes from soil reflectance data, produce dense databases that require large processing capacities.

Another soil aspect dependent on numerous variables is its classification from a pedogenic point of view. This has been the subject of several studies using proximal sensors, such as done by Xie and Li (2018), that aimed to predict soil classes through their spectral characteristics. The fact that the spectrally active components of the soil in the visible and near infrared (Vis-NIR) regions are mainly iron oxides, organic matter, clay minerals, carbonates and water (Ben-Dor, 2002; Stenberg et al., 2010) has allowed the use of spectrometry in integrative analyzes (Awiti et al., 2008), from soil quality (Askari et al., 2015) to its classification (Rossel and Webster, 2011; Ogen et al., 2017).

However, the problem with the high density of the databases generated by analyzes performed with proximal sensors still persists. As one of the alternatives, the principal components analysis (PCA) transforms high density datasets into components representing the initial data, having a smaller size and preserving the data variability as much as possible (Jollife and Cadima, 2016; Wu et al., 2018).

The use of PCA in geoenvironmental studies, with emphasis on soil science, has enabled studies such as the one done by Nketia et al. (2019), that used PCA to develop a methodology for selecting sampling points that were representative of soil properties of interest and soil-landscape interactions. Another example of the use of PCA, was the selection of variables to construct a model for predicting soil physical properties developed by Levi and Rasmussen (2014) and its use to evaluate soil contamination levels by heavy metal near copper mines (Zhiyuan et al., 2011).

The possibility of using PCA, regression trees, machine learning, neural networks, among other statistical and computational techniques associated with new soil evaluation methodologies such as reflectance spectroscopy (Demattê and Terra, 2014; Rossel et al., 2016; Moura-Bueno et al., 2019), open possibilities for the characterization and assessment of soils and their formation environments.

In this way, the purpose of this study was to evaluate the separation of soil classes from spectral reflectance data using principal components analysis.

2. Materials and Methods

The study was conducted in the Aiuaba Experimental Basin (BEA), located in the municipality of Aiuaba, in the State of Ceará, northeast region of Brazil. BEA is inserted in the Upper Jaguaribe Basin, and is currently considered the largest Federal reserve of the Caatinga biome. The basin area has approximately 12 km² (Figure 1) and it is fully inserted in an ecological station, which means that it is a preserved area.

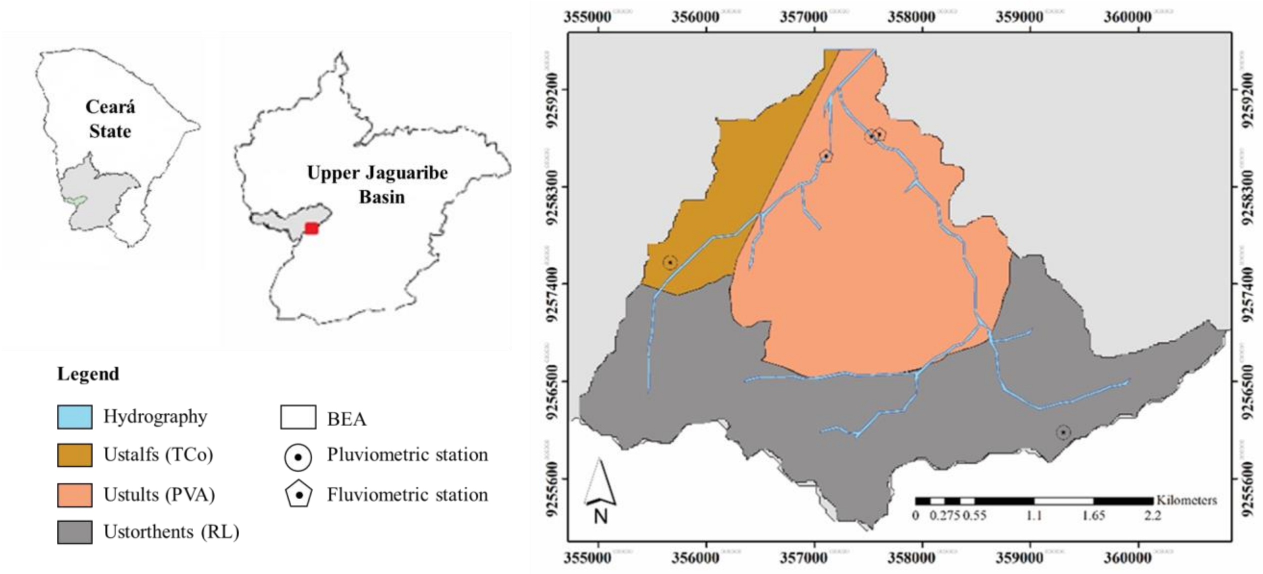

Figure 1 - Aiuaba Experimental Basin (BEA), its location in the State of Ceará, and in the Upper Jaguaribe Basin, with the distribution of soil classes and basin hydrography.

The climate of the region is defined as 'Bs' according to the Köppen's classification, presenting average precipitation of 560 mm year^{-1} and evaporation of 2,500 mm year^{-1} by class A tank (Araújo and González Piedra, 2009).

Based on the assessment of the environmental dynamics in this basin, the area was divided into three associations between soil and vegetation (ASVs) that were defined as homogeneous units for studies of the environmental variables. Pinheiro et al. (2016) and Costa et al. (2013) classified the ASVs based on their predominance of soil and vegetation, which are presented in Table 1.

Table 1 - Study area description.

ASV	Predominant vegetation	Soil class	Area in BEA (%)
ASV1	Catingueira (*Caesalpinia pyramidalis* Tul)	Ustalfs (TCo)	20
ASV2	Angelim (*Piptadenia obliqua*)	Ustults (PVA)	34
ASV3	Jurema-preta (*Mimosa tenuiflora* (Willd.) Poir)	Ustorthents (RL)	46

Source: Pinheiro et al. (2016).

Four soil samples were collected in characteristic profiles at each ASV. The samples were collected at a soil depth of 0-0.2 m. Subsequently, they were stored and identified for further analysis. Analyzes were carried out to determine the texture (pipette method) and organic matter (OM, wet-oxidation with potassium dichromate) content according to the methodology presented in Teixeira et al. (2017). The analyzes were carried out at the Soil Laboratory of the Embrapa Agroindústria Tropical (Fortaleza, Ceará State, Brazil).

In order to obtain the soil reflectance data using a proximal sensor, the FieldSpec 3 sensor was used according to the methodology of Romero et al. (2018). This sensor has a resolution of 1 nm (350-1100 nm) and 2 nm (1000-2200 nm). The system geometry was based on the perpendicular positioning of the sensor in relation to the sample, maintaining a distance of 6 cm. The light source was positioned at 50 cm from the sample, forming a 45° angle with the zenith. A white spectral plate was used as the spectral standard reference. The reflectance values were obtained from the average of three readings for each sample.

After obtaining the data, they were submitted to principal component analysis (PCA), using the software R (R Core Team, 2019) and the FactorMaineR package scripts provided by Lê et al. (2008), in order to identify the most important components and the separation of the soil classes. This technique was used to evaluate the importance of the 2,500 reflectance bands analyzed by the spectroradiometer and identify which of them contribute more significantly to the separation of the soil classes analyzed, based on their relationship with the soil attributes.

To perform the selection of the number of CPs were considered those with eigenvalue higher than the unit. This criterion is based on the fact that any component must explain a variance greater than that presented by a single standardized variable (band), as explain Hair et al. (2009).

3. Results and discussion

The results of the textural class and OM analysis can be observed in Table 2.

The highest OM contents were observed in the Ustults, while the lowest were in the Ustorthents. A highlight is given to the silt content of Ustalfs, which may be associated with its poor pedogenetic development. The highest sand contents, as expected, were observed in the Ustorthents.

Organic matter is characterized in the range of 750-870 nm, its chromophore characteristic is mainly given by the combination C-H, N-H, O-H and the vibration of these elements (Xie and Li, 2018). Moura-Bueno et al. (2019), using spectral characteristics modeling to predict soil organic carbon (SOC), observed that bands between 400-800 nm were responsible for explaining the greater variability of this soil attribute. This range has also been observed in studies developed by Vasques et al. (2008), Rossel et al. (2016) e Jiang et al. (2017), and has been described as an important region in spectral curves associated with land use, soil class and SOC content (Moura-Bueno et al., 2019).

Table 2 - Texture and organic matter, and their deviations, for the three soil classes analyzed.

ASV	Soil class	Organic Matter (kg kg^{-1})	Texture (kg kg^{-1})			
			Fine sand	Coarse sand	Silt	Clay
ASV1	Ustalfs	0.015 (±0.001)	0.191 (±0.003)	0.170 (±0.009)	0.455 (±0.008)	0.183 (±0.005)
ASV2	Ustults	0.031 (±0.007)	0.204 (±0.004)	0.152 (±0.004)	0.313 (±0.004)	0.329 (±0.002)
ASV3	Ustorthents	0.012 (±0.004)	0.321 (±0.003)	0.350 (±0.004)	0.240 (±0.004)	0.090 (±0.002)

The reflectance of each soil class is based on their pedogenetic development, and how this process influenced the distribution of soil properties, such as their clay fraction, and granulometry (Demattê and Terra, 2014). The predominant presence of specific minerals, for example, reflects the weathering state of the soil. The class of Ustuls presents mineralogy predominantly formed by kaolinite, feldspars, illite, and quartz (Lima et al., 2008; Brighenti, et al., 2012) while Ustorthents present also pyroxenes, olivines, and plagioclases in the clay fraction (Pedron et al., 2012). In Ustalfs, because they are high-active clay soils, a predominance of smectites and vermiculites is expected (Araújo, 2000; Corrêa et al., 2003).

In relation to the spectral response curves of the soils obtained with the proximal sensor, the soil classes of the three ASVs presented a quite different behavior as can be observed in Figure 2.

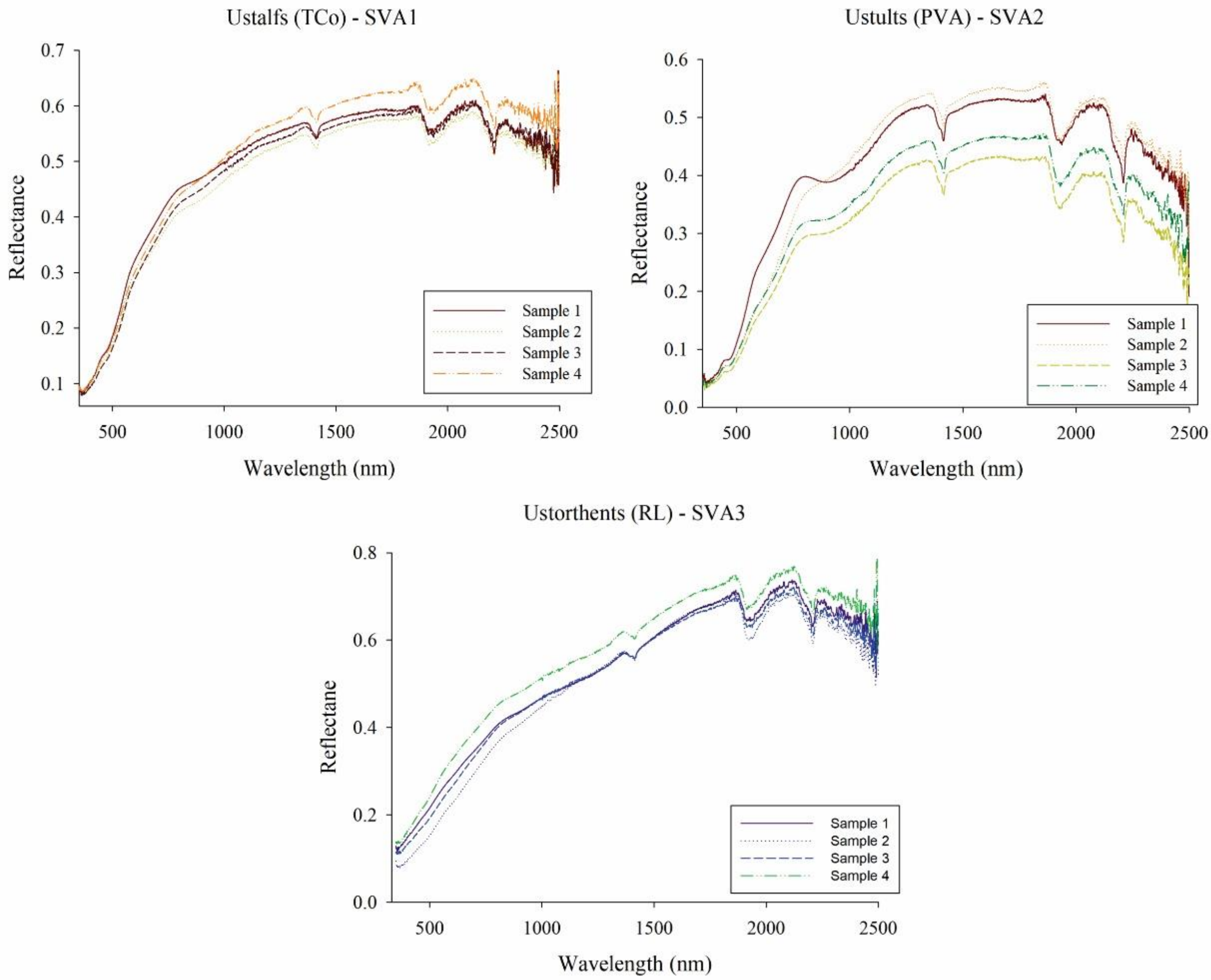

Figure 2 - Spectral curve of the soil classes obtained with proximal sensor.

It was observed a greater homogeneity of spectral response for the Ustalfs samples, greater distinctions were observed only after the wavelength of 1350 nm. On the other hand, the other two classes showed a greater heterogeneity of responses at most wavelengths.

Regarding the separation of the wavelengths that compose the soil reflectance, the separation of the data set from the reflectance observed in the analyzed bands was grouped into different principal components (PCs), as shown in Figure 3.

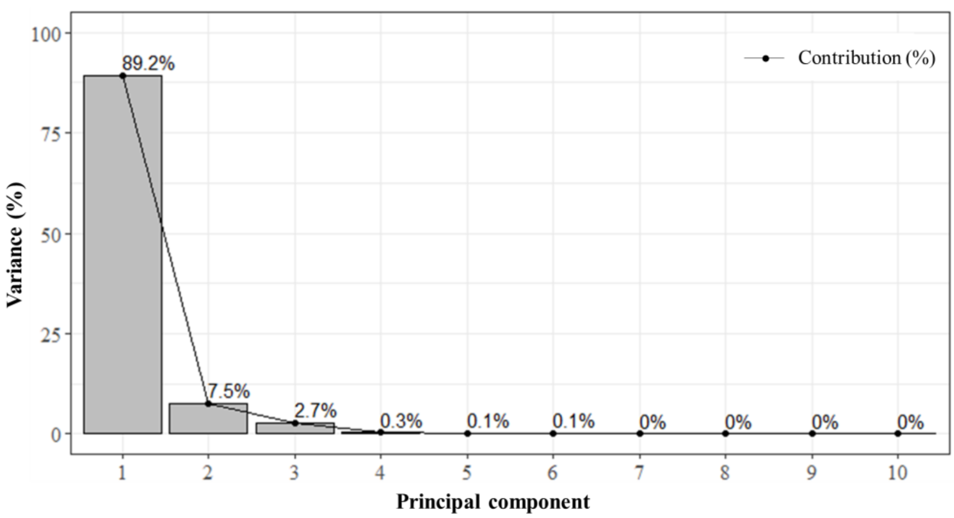

Figure 3 - Variance contained in the first ten principal components of the reflectance spectrum of the soils and the contribution of each PC.

It was observed that the greatest variability of the data is inserted in the first principal component, and significant variability is observed until the third PC, explaining 99.4% of the variation of the total spectral data. The contribution of the number of reflectance bands in the construction of the PCs is strongly concentrated in the first two components, which indicates a low contribution in the variability when considering the spectral data that constitute the other main components.

In Table 3 are presented, in descending order, the bands (wavelengths) that most contributed to explaining the variability of the tree firsts PCs. It is possible to realize that different band ranges are responsible to better explain each PC, highlighting the ability of PCA to identify the variables that distinguish each of the main components defined.

Table 3 - Bands that most contributed to explain the variability of the PC1, PC2 and PC3.

Rank	PC1		PC2		PC3	
	Band (nm)	**Contribution (%)**	**Band (nm)**	**Contribution (%)**	**Band (nm)**	**Contribution (%)**
1º	1415	0.05143	756	0.1751	356	0.2510
2º	1418	0.05143	760	0.1751	387	0.2243
3º	1417	0.05142	755	0.1750	382	0.2203
4º	1414	0.05142	752	0.1748	357	0.2201
5º	1416	0.05141	762	0.1748	384	0.2158
6º	1421	0.05139	753	0.1746	381	0.2154
7º	1419	0.05139	750	0.1745	434	0.2116
8º	1420	0.05139	751	0.1744	446	0.2109
9º	1413	0.05138	757	0.1743	433	0.2102
10º	1412	0.05134	754	0.1742	441	0.2100

After the treatment of the spectral data through the PCA, the first three PCs were used to separate the soil classes using the two-dimensional graphical analysis (Figure 4).

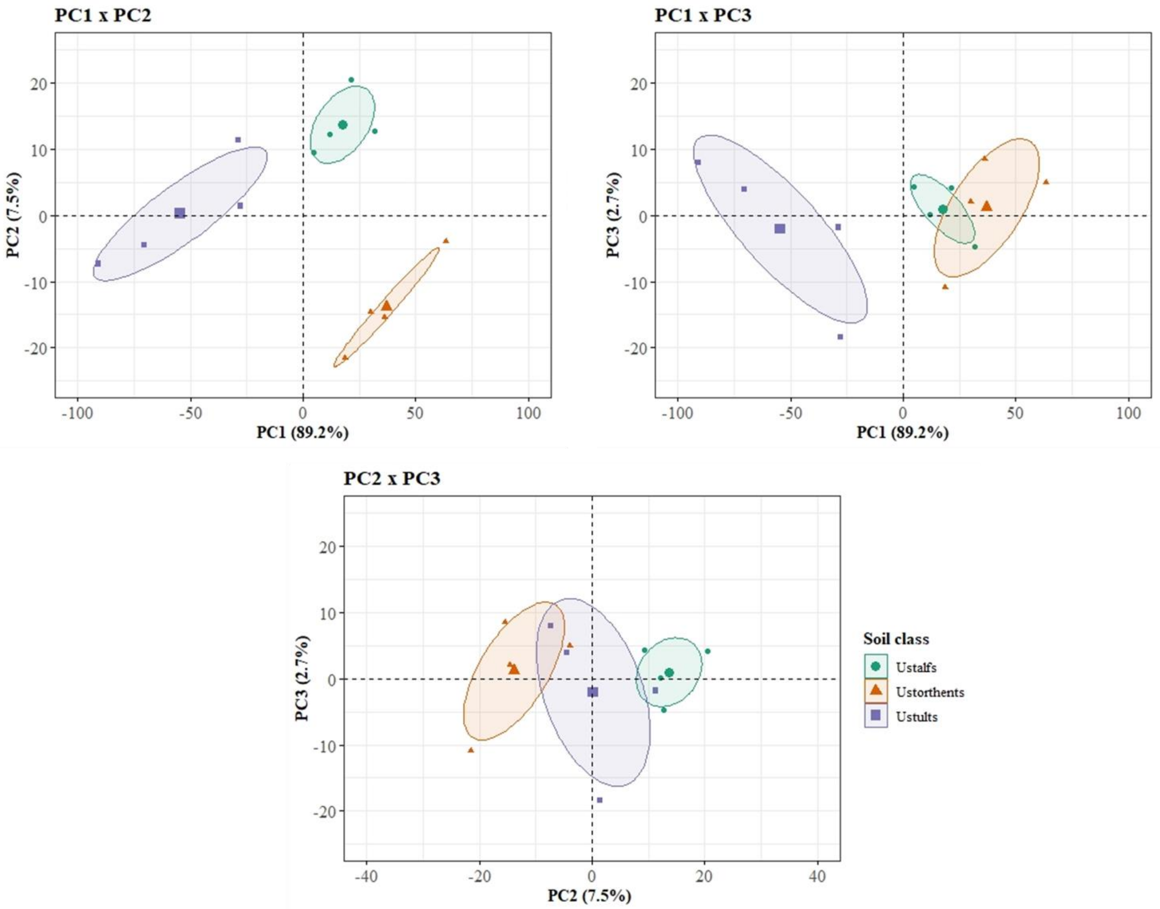

Figure 4 - Two-dimensional analysis of the spectral data of Ustalfs, Ustults and Ustorthents.

It can be observed in the comparison between the first two PCs (PC1 x PC2) that the spectral data are sufficiently discriminatory to perform the separation between the Ustalfs, Ustults, and Ustorthents. The distinction between Ustorthents and Ustalfs was not well performed in the other two-dimensional analyzes (PC2 x PC3 and PC1 x PC3). It was observed that in the analyzes between PCs with lower variance contribution (PC2 x PC3), the separation of soil classes was not satisfactory.

The selective absorption by the soil components, mainly iron oxides, OM, and the constituents of the clay fraction, make possible the use of Vis-NIR in the evaluation of soil properties (Ben-Dor, 2002; Xie; Li, 2018). The wavelengths that presented the greatest contribution in the formation of the three principal components were the intervals of 1412-1420; 750-760 and 350-380 nm, respectively (Table 3). These wavelengths are mainly associated with the reflectance of clay minerals, 1:1 (kaolinite), and 2:1 (smectite, mica, and illite) which have a strong signal between 1400-2200 nm, as affirm the authors Ben-Dor (2002) and Demattê and Terra (2014). These same authors also pointed out the importance of residual water present in the soil and in the 1:1 and 2:1 clay mineral that intensifies this spectral response.

Therefore, when the greatest variability in the PC1 is observed (Figure 3), this variation should be associated with greater heterogeneity of reflectance in the range of 1350-1450 nm, in all the samples evaluated (Figure 2), which corroborates with the bands that contributed the most in the construction of the first component, which certainly cooperated for the distinction of soil classes in the two-dimensional analysis.

The range of 380-430 nm and 480-550 nm are absorption ranges characteristic of iron oxides such as hematite and goethite (Sherman and Waite, 1985; Parikh et al., 2014) which have their formation in the soil conditioned to climatic characteristics and are responsible for soil attributes, such as their color.

The Ustorthents class, which presented differentiation in the reflectance curve and in the two-dimensional analysis, is characterized by a higher albedo response and thus an upward growth of its curve (Figure 2) as well as an increased reflectance near the infrared (SWIR, 1200-2500 nm), which could explain the lower amount of iron oxides and the higher amounts of quartz present in the soil (Romero et al., 2018).

The separation of all the classes using PC2 and PC3 was not possible due to the low accumulated variability of their constituents, whereas the non-separation of Ustorthents and Ustalfs may be associated to the spectral behavior of the soils in the range 350-450 nm that contributed more strongly to the construction of PC3. This range makes the characterization of iron oxides, and due to the incipient degree of pedogenetic development of the classes (Oliveira et al., 2008, 2009), the reflectance variation may not have been representative enough for the separation.

5. Conclusions

From the use of spectral behavior data of different soil classes submitted to principal components analysis it was identified that the reflectance intervals that refer to clay minerals (1412-1420), organic matter (750-760) and iron oxides (350- 380) were the main responsible for explaining the variability of the principal components. Therefore, using the spectral characterization data that showed greater variability submitted to PCA, it was possible to separate the classes Ustorthents, Ustalfs and Ustults from each other.

Acknowledgment

The authors would like to thank the Brazilian Agricultural Research Corporation (Embrapa), the Federal University of Viçosa (UFV) and the Coordination for the Improvement of Higher Education Personnel (CAPES - Financial Code 001).

References

Araújo, J.C.de, González Piedra, J.I., 2009. Comparative hydrology: analysis of a semiarid and a humid tropical watershed. Hydrological Processes 23, 1169–1178.

Araújo, M.doS.B., 2000. Fósforo em toposseqüências de Latossolos e Luvissolos do semi-árido de Pernambuco. Lavras: Universidade Federal de Viçosa.

Askari, M.S., O'rourke, S.M.; Holden, N.M., 2015. Evaluation of soil quality for agricultural production using visible-near-infrared spectroscopy. Geoderma 243–244, 80–91.

Awiti, A.O., Walsh, M.G., Shepherd, K.D., Kinyamario, J., 2008. Soil condition classification using infrared spectroscopy: A proposition for assessment of soil condition along a tropical forest-cropland chronosequence. Geoderma 143, 73-84.

Ben-Dor, E., 2002. Quantitative remote sensing of soil properties. Advances in Agronomy 75, 173-244.

Brighenti, I., Almeida, J.A., Hofer, A., 2012. Mineralogia e gênese de argissolos das serras do Tabuleiro/Itajaí, Estado de Santa Catarina. Revista Brasileira de Ciência do Solo 36, 1057–1071.

Cheng, H., Shen, R., Chen, Y., Wan, Q., Shi, T., Wang, J., Wan, Y, Hong, Y., Li, X., 2019. Estimating heavy metal concentrations in

suburban soils with reflectance spectroscopy. Geoderma 336, 59–67.
Corrêa, M.M., Ker, J.C., Mendonça, E.S., Ruiz, H.A., Bastos, R.S., 2003. Atributos físicos, químicos e mineralógicos de solos da região das Várzeas de Sousa (PB). Revista Brasileira de Ciência do Solo 27, 311–324.
Costa, C.A.G., Lopes, J.W.B., Pinheiro, E.A.R., Araújo, J.C.D., Gomes Filho, R.R., 2013. Spatial behaviour of soil moisture in the root zone of the Caatinga biome. Revista Ciência Agronômica 44, 685-694.
Curcio, D., Ciraolo, G., D'Asaro, F., Minacapilli, M., 2013. Prediction of soil texture distributions using VNIR-SWIR reflectance spectroscopy. Procedia Environmental Sciences 19, 494–503.
Demattê, J.A.M., Terra, F.S., 2014. Spectral pedology: A new perspective on evaluation of soils along pedogenetic alterations. Geoderma 217–218, 190–200.
Hair, J.F., Black, W.C., Babin, B.J., Anderson, R.E., Tatham, R.L., 2009. Análise Multivariada de Dados. São Paulo: Bookman Editora.
Jiang, Q., Li, Q., Wang, X., Wu, Y., Yang, X., Liu, F., 2017. Estimation of soil organic carbon and total nitrogen in different soil layers using VNIR spectroscopy: Effects of spiking on model applicability. Geoderma 293, 54–63.
Jolliffe, I.T., Cadima, J., 2016. Principal component analysis: a review and recent developments. Philosophical Transactions of the Royal Society A: Mathematical, Physical and Engineering Sciences 374, 2065, 20150202.
Kalambukattu, J.G., Kumar, S., Arya Raj, R., 2018. Digital soil mapping in a Himalayan watershed using remote sensing and terrain parameters employing artificial neural network model. Environmental Earth Sciences 77, 203.
Laborczi, A., Szatmári, G., Takács, K., Pásztor, L., 2016. Mapping of topsoil texture in Hungary using classification trees. Journal of Maps 12, 999–1009.
Lê, S., Josse, J., Husson, F., 2008. FactoMineR: An R Package for Multivariate Analysis. Journal of Statistical Software 25, 1.
Levi, M.R., Rasmussen, C., 2014. Covariate selection with iterative principal component analysis for predicting physical soil properties. Geoderma 219, 46–57.
Liddicoat, C., Maschmedt, D., Clifford, D., Searle, R., Herrmann, T., Macdonald, L. M., Baldock, J., 2015. Predictive mapping of soil organic carbon stocks in South Australia's agricultural zone. Soil Research 53, 956–973.
Lima, J.G.D.C., Schulze, S.M.B.B., Ribeiro, M.R., Barreto, S.D.B., 2008. Mineralogia de um argissolo vermelho-amarelo da zona úmida costeira do estado de Pernambuco. Revista Brasileira de Ciência do Solo 32, 881-892.
Mendonça-Santos, M.D.L., Dart, R.D.O., Santos, H.G., Coelho, M.R., Berbara, R.L.L., Lumbreras, J.F., 2010. Digital Soil Mapping of Topsoil Organic Carbon Content of Rio de Janeiro State, Brazil, in: Digital Soil Mapping. Dordrecht: Springer Netherlands, pp. 255–266.
Moura-Bueno, J.M., Dalmolin, R.S.D., Ten Caten, A., Dotto, A.C., Demattê, J.A., 2019. Stratification of a local VIS-NIR-SWIR spectral library by homogeneity criteria yields more accurate soil organic carbon predictions. Geoderma 337, 565–581.
Nketia, K. A., Asabere, S. B., Erasmi, S., Sauer, D., 2019. A new method for selecting sites for soil sampling, coupling global weighted principal component analysis and a cost-constrained conditioned Latin hypercube algorithm. MethodsX 6, 284-299.
Ogen, Y., Goldshleger, N., Ben-Dor, E., 2017. 3D spectral analysis in the VNIR–SWIR spectral region as a tool for soil classification. Geoderma 302, 100–110.
Oliveira, L.B.D., Fontes, M.P.F., Ribeiro, M.R., Ker, J.C., 2008. Micromorfologia e gênese de Luvissolos e Planossolos desenvolvidos de rochas metamórficas no semi-árido brasileiro. Revista Brasileira de Ciência do Solo 32, 6, 2407-2423.
Oliveira, L.B.D., Fontes, M.P.F., Ribeiro, M.R., Ker, J.C., 2009. Morfologia e classificação de Luvissolos e Planossolos desenvolvidos de rochas metamórficas no semiárido do nordeste brasileiro. Revista Brasileira de Ciência do Solo 33, 1333-1345.
Parikh, S.J., Goyne, K.W., Margenot, A.J., Mukome, F.N., Calderón, F.J., 2014. Soil Chemical Insights Provided through Vibrational Spectroscopy. Advances in Agronomy 126, 1–148.
Pedron, F.A., Azevedo, A.C.de, Dalmolin, R.S.D., 2012. Alteração mineralógica de neossolos em uma climo-litossequência no planalto do rio grande do sul. Ciencia Rural 42, 451–458.
Pinheiro, E.A.R., Metselaar, K., Jong van Lier, Q.de, Araújo, J.C.de, 2016. Importance of soil-water to the Caatinga biome, Brazil. Ecohydrology 9, 1313–1327.
R Core Team., 2019. A language and environment for statistical computing**.** R Foundation for Statistical Computing, Vienna, Austria. Disponível: https://www.r-project.org/. Acesso:
Romero, D.J., Ben-Dor, E., Demattê, J.A., Souza, A.B., Vicente, L.E., Tavares, T.R., Martello, M., Strabeli, T.F., Barros, P.P.S., Fioro, P.R., Gallo, B.C.; Sato, M.V., Eitelwein, M.T., 2018. Internal soil standard method for the Brazilian soil spectral library: Performance and proximate analysis. Geoderma 312, 95-103.
Rossel, R.A.V., Webster, R., 2011. Discrimination of

Australian soil horizons and classes from their visible-near infrared spectra. European Journal of Soil Science 62, 637–647.

Rossel, R.V., Behrens, T., Ben-Dor, E., Brown, D.J., Demattê, J.A.M., Shepherd, K.D., Shi, Z., Stenberg, B., Stevens, A., Adamchuk, V., Aïchi, H., Barthès, B.G., Bartholomeus, H.M., Bayer, A.S., Bernoux, M., Böttcher, K., Brodský. L., Du, C.W., Chappell, A., Fouad, Y., Genot, V., Gomez, C., Grunwald, S., Gubber, A.; Guerrero, C., Hedley, C.B., Knadel, M., Morrás, H.J.M., Nocita, M., Ramirez-Lopez, L., Roudier, P., Campos, E.M.R., Sanborn, P., Sellitto, V.M., Sudduth, K.A., Rawlins, B.G., Walter, C., Winowiecki, A., Hong, S.Y., Ji, W., 2016. A global spectral library to characterize the world's soil. Earth Science Reviews 155, 198–230.

Sherman, D.M., Waite, D.T., 1985. Electronic spectra of Fe^{3+} oxides and oxide hydroxides in the near IR to near UV. American Mineralogist 70, 1262–1269.

Stenberg, B., Rossel, R.A.V., Mouazen, A.M., Wetterlind, J., 2010. Visible and near infrared spectroscopy in soil science, in: Advances in Agronomy. Burlington: Academic Press, pp.163-215.

Teixeira, P.C., Donagemma, G.K., Fontana, A., Teixeira, W.G., 2017. Manual de Métodos de Análise de Solo. Rio de Janeiro: Embrapa.

Vasques, G.M., Grunwald, S., Sickman, J.O., 2008. Comparison of multivariate methods for inferential modeling of soil carbon using visible/near-infrared spectra. Geoderma 146, 14–25.

Xie, X., Li, A., 2018. Identification of soil profile classes using depth-weighted visible-near-infrared spectral reflectance. Geoderma 325, 90–101.

Wu, X., Wai, H., Li, L., Scaglione, A., 2018. A Review of Distributed Algorithms for Principal Component Analysis. Proceeding of the IEEE 106, 1321–1340.

Zhiyuan, W., Dengfeng, W., Huiping, Z., Zhiping, Q.I., 2011. Assessment of Soil Heavy Metal Pollution with Principal Component Analysis and Geoaccumulation Index. Procedia Environmental Sciences 10, 1946–1952.